IUST
Iran University of Science and Technology

Iranian Journal of Electrical and Electronic Engineering

Journal Homepage: ijeee.iust.ac.ir

Review Paper

A Review on the Power Circuit Topologies of Current Source Inverters in Photovoltaic Applications

N. Danapour*(C.A.), E. Akbari**, and M. Tarafdar-Hagh*

Abstract: In electricity generation through photovoltaic cells, efficient inverters are required to inject the generated power into the grid. Among the inverters connected to the grid, current source inverters despite their advantages are used less than voltage source ones. Different circuits are presented for these converters. In this paper, several power circuit topologies of the current source inverters, which are an interface between solar panels and the grid, are reviewed. Also, the inverters are compared from the point of some indexes like efficiency, voltage transmission ratio, total harmonic distortion, leakage currents, and their reduction methods. The importance of these indexes is investigated too. Categorization is for full-bridge inverters and special structures groups. The first group includes the conventional inverter, 4-leg inverter, CH7 CSI, H7 CSI, three-mode, and other structures. The second group consists of inverters with special structures and is independent of the conventional CSI. The summary of the studies is presented in a table.

Keywords: Current Source Inverters, Full-Bridge Inverters, Leakage Current, Photovoltaic Systems, THD, Transformer-less PV System.

1 Introduction

PHOTOVOLTAIC (PV) technology, due to its reliability and availability, has been one of the most interested among renewable technologies, and recently PV systems' cost is decreased [1-3]. Despite the mentioned advantages, solar panels usually provide low-level dc voltage to inverters' input [4, 5]. As a result, these systems are used to supply low and medium-voltage grids, that this feature is considered as a drawback for PV systems. Therefore, the voltage amplification feature is a notable benefit for converters as enables PV systems to supply higher voltage grids [6, 7]. PV system is a converter-based technology, and converters play an important role in power injection from PV into the grid and influence voltage, frequency, and power quality of the power system. Accordingly, they seem to be the primary universal modular building block for future smart grids, especially at medium and low voltage [8-10]. The primary failures of PV systems are converter failures. Thus, selecting the best inverter according to its parameters has deep impacts on the increasing efficiency, reliability, and decreasing the final cost, mainly in the future hybrid energy system and micro-grid systems, where the inverter technologies have an important influence on the price of distributed systems [1, 11, 12]. The utility of inverters is not only limited to the mentioned applications, but also widely used inverters in the Flexible AC Transmission Systems (FACTS) and wind farms [13]. The improvement of converters significantly influences the power systems and related research. Thus, it seems to be an important part of future power system studies. The inverters which are used in the photovoltaic are divided into two categories:

1. Voltage source inverters (VSI),
2. Current source inverters (CSI).

VSIs, due to their simplicity and reliability, are used extensively in renewable energy applications. However, due to the voltage reduction feature, they require a boost

Iranian Journal of Electrical and Electronic Engineering, 2022.
Paper first received 24 January 2022, revised 05 April 2022, and accepted 01 May 2022.
* The authors are with the Department of Electrical and Computer Engineering, University of Tabriz, Tabriz, Iran.
E-mails: nasserdanapour@gmail.com and tarafdar@tabrizu.ac.ir.
** The author is with the Department of Electrical and Computer Engineering, Mazandaran University of Science and Technology, Mazandaran, Iran.
E-mail: akbari.ehsan101@gmail.com.
Corresponding Author: N. Danapour.
https://doi.org/10.22068/IJEEE.18.3.2404

DC-DC converter or large-scale transformer [14]. One of the main concerns about the boost converters is their efficiency [15]. In addition, VSIs use a high-value electrolytic capacitor in dc side that is a weak link in the system [16], and it causes some limitations such as:

1. Due to the use of DC-DC boost inverter, the efficiency reduces, and the number of components increases. So the cost of the system increases.
2. Power conversion is done in two stages (DC-DC and DC-AC). Accordingly, the power conversion efficiency is low.
3. Using more components reduces reliability.
4. The size and weight of the system increase.
5. Extremely can be affected by electromagnetic interference (EMI) noise [17].

While the current source inverters have the voltage-boost feature, they can connect the low-level voltage PVs to the grid. Also, CSIs have other advantages compared to VSIs, such as continuous output current, using the series inductor at the input instead of a high-value capacitor in the DC-Link that improves the reliability, especially in short-circuit conditions [16, 18]. CSI has a smaller capacitor on the output side, and power conversion is done in single-stage, so the system's reliability is increased. However, it must be noted that the control system of CSIs is more complex in comparison to VSIs [19, 20]. A summary comparison of VSI and CSI is presented in Table 1. The conventional topology of CSIs is based on the full-bridge inverter; however, there are different types of CSI topologies. Reference [21] proposes 4-leg inverters to reduce the leakage current using an inductor at the input, and in [22] has been proven that its reliability is more than VSI and conventional ones. This inverter has eight bridges and two capacitors on the DC link. In [23, 24], a Tri-stage inverter is proposed to reach the higher Voltage Transmission Ratio (VTR). In addition, this structure has a good dynamic response. The proposed inverter in [25] uses the presented method in [23] for a single-phase state. As it uses bypass switches at the two sides of the input inductor to control the stored energy. Accordingly, the mentioned approach causes an increase in inverter efficiency. In CH7 power circuit, which is proposed in [26], there is a parallel switch to the legs of the inverter, which did not exist in the conventional CSI. The mentioned switch is used for reducing leakage current. A similar method is used in [27] for a single-phase state. A passive filter is implemented on the DC side of inverters in [20] to limit the second-order and fourth-order harmonics from the input current. For this purpose, three inductors and two capacitors are used in the input filter. However, there is no information about the power density and complexity of the circuit and its efficiency. The structures outlined in [28, 29] eliminate the power ripple with twice the line frequency from the DC side. Despite the benefits provided by [28, 29] structures, they cause an increase in the number of switches, cost, and complexity of the inverter. Also, the inverter of paper [29] is not able to compensate the power ripple in the fault situation. Total Harmonic Distortion (THD) of the inverter proposed in [28] is more than the reference [30] and [31] inverters' THD. The presented inverter in [31] can provide buck, boost and buck-boost type of operation so cause to complete maximum power point tracking (MPPT). This inverter works in discrete directivity mode to reduce inverters weight and volume, this reason causes to increase the maximum of input current. In addition, it has low VTR, so it is useful for low voltage applications. The CSI5 inverter in [32] decreases the amount of leakage current. However, the number of switches and power loss are increased in that structure. Also, some of its switches connect and disconnect in hard switching conditions. Moreover, the mentioned structure based on full-bridge inverters, there are inverters with a special structure. A three-phase inverter is one of these specials that is proposed in [33]. This inverter is able to generate voltages less and more than the input voltage. In this paper, the provided structures for current source inverters used for the connection of PV to the grid are investigated. At first, the comparison indexes are introduced, and in the next part, full-bridge-based CSIs and inverters with the special structure are categorized and explained. Finally, the results are provided in a summary table.

2 Comparison Indexes

In order to compare different convertors provided in references, some indexes are considered. The mentioned indexes are as below.

Table 1 Summary comparison of VSI and CSI.

Comparison criteria	Voltage source inverter	Current source inverter
DC-link value	$V_{dc} = \sqrt{3}V_{phase,\ peak}$	$I_{dc} \geq I_{phase,\ peak}$
Cost and sizing DC component	DC capacitor is small, cheap, and efficient energy storage.	DC inductor is bulky, expensive, and contributes more losses.
Steady-state and transient response	Good steady-state performance. Excellent response during transient with small overshoot.	Good steady-state performance. However, takes longer time to reach steady-state. Satisfactory performance during transient.
Power semiconductor losses	High switching loss but low conduction loss. Thus, total power loss is low. At high switching frequency, the total loss is higher than CSI.	Low switching loss but high conduction loss. Thus, the total power loss is high. However, at high switching frequency, the total loss is lower than VSI.

2.1 Inverter Voltage Gain

As referred before, CSIs can operate as step-up converters. Consequently, less solar plate is needed for CSIs with higher voltage gains.

2.2 Ability of Maximum Power Point Tracking (MPPT)

Solar plates can generate maximum generable power at a special amount of output voltage at each moment. By changing environmental conditions, the amount of the referred voltage or the current related to the maximum power point changes [34], so the inverter must be capable of tracking the maximum power point.

2.3 THD of Output Current

THD of output current is most often generated by nonlinear devices. THD limits are presented in IEEE-519 standard. To not drop down the output power quality, the amount of THD must not exceed standard levels [35].

2.4 Leakage Current

Metal plates are used to improve the mechanical strength of photovoltaic modules. Because of the overlap between the module and metal plates, a capacitor appears between them. These plates are connected to the earth because of safety, so a parasitic capacitor is made between the earth and the side of the photovoltaic module. The amount of mentioned capacitors is changed by changing environment temperature, humidity, dust, etc. This value range for glass-faced panels is between 50 and 150 nF/kWp, however, it can reach 1 μF/kWp in rainy and humid environment condition for tin-film panels. The inverter output can be connected to a grid via an isolation transformer, and by connecting module terminals to the ground, the voltage will be double-headed for DC parasitic capacitors, and there will be no flow of this capacitor to the ground. But in the direct connection of the inverter to PV terminals, they cannot be connected to the ground. Because the grid null is connected to the ground, the potential differences between the PV and the grid terminals depend on the direction of the inventor keys, and this causes a fault flow through the ground. On the other hand, in the absence of low PV terminals, high voltage switching voltages will be generated on both sides of the parasitic capacitors, resulting in leakage currents. Parasitic capacitors are modeled as $Cp1$ and $Cp2$ in Fig. 3 [36-40].

2.5 Power Losses

Power losses in inverters include loss of conduction mode and switching of semiconductor elements, core losses of transformers and inductors, as well as power losses in resistances equivalent to inductors and circuit capacitors. These should be minimized as much as possible. For example, soft-switching methods can be used to reduce switching losses.

2.6 Efficiency

One of the most important indicators for evaluating the inverter is the efficiency of the system. Based on European Union (EU) and California Energy Commission (CEC) efficiencies, the efficiency of the grid-connected inverters should not be less than 95% [41].

2.7 Semiconductor Elements

One of the factors affecting the inverter costs is the number of keys that are also related to the amount of losses. Converters often use either the Insulated Gate Bipolar Transistor (IGBT) or Metal Oxide Semiconductor Field Effect Transistor (MOSFET) semiconductor switches according to their working parameters. Specifications for using these semiconductors are listed in Table 2 [42].

2.8 Size and Number of Passive Elements

This factor has a significant effect on the inverter power density, as well as the cost of its construction and maintenance. In addition, high electrolytic capacitors reduce reliability. Recently researchers have tried to reduce the number of passive components to achieve low-cost systems [43].

2.9 Switching Frequency

The use of high-frequency switching in grid-connected converters reduces the inductance value and output current harmonics; therefore, the output filter design for generating quality output waveform will be more accessible [12, 42]. However, the switching loss and sampling frequency are the limiting parameters for switching frequency [20].

With regarding the mentioned contents, Inverters used as interfaces between solar panels and the grid should have some features such as low THD, as well as the direct input current stream, which improves MPPT, has the advantage of converting, the possibility of getting

Table 2 Specifications of MOSFET and IGBT [42].

Switch	Power range	Switching frequency [kHz]	Advantage	Disadvantage
MOSFET	Low power < 10 kW	20–800	High-frequency switching	Low power
IGBT	Medium to high power > 100kW	< 20	High power	Low-frequency switching

Table 3 Standards that are important in PV applications [45].

Standard	Scope and object
IEC 61727	Applies to utility-interconnected photovoltaic (PV) power systems operating in parallel with the utility and utilizing static (solid-state) non-islanding inverters for the conversion of DC to AC. Lays down requirements for interconnection of PV systems to the utility distribution system.
EN 61000-3-2	Deals with the limitation of harmonic currents injected into the public supply system. It specifies limits of harmonic components of the input current which can be produced by equipment tested under specified conditions. It is applicable to electrical and electronic equipment having a rated input current up to and including 16 A per phase, and intended to be connected to public low-voltage distribution systems.
IEEE 1547	The technical specifications for, and testing of, the interconnection and interoperability between utility electric power systems (EPSs) and distributed energy resources (DERs) are the focus of this standard. It provides requirements relevant to the performance, operation, testing, safety considerations, and maintenance of the interconnection. It also includes general requirements, response to abnormal conditions, power quality, islanding, and test specifications and requirements for design, production, installation evaluation, commissioning, and periodic tests.
U.S. National Electrical Code (NEC) 690	The Code specifies how to safely do electrical work. The Code is updated every few years to include new technology and improved safety practices.
IEEE 519-2014	This standard defines the voltage and current harmonics distortion criteria for the design of electrical systems. Goals for designing electrical systems that contain both linear and non-linear loads are established in this standard. The existed voltage and current waveforms in every part of the system are explained, and the waveform distortion goals for the system designer are established.

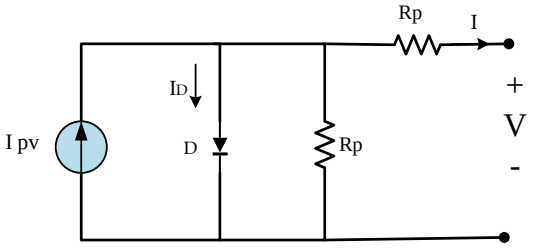

Fig. 1 Single diode RP model.

maximum power from a solar panel and so on.

2.10 Standards

Appropriate standards are determined by international organizations to deal with issues like power quality, detection of islanding operation, grounding, etc. Some of the standards that are important in PV applications are presented in Table 3.

3 Modeling of PV Cells and Configurations of Inverters and Arrays in PV Applications

PV cells can be simulated in a variety of ways, an appropriate PV cell circuit model is one that accurately simulates the electrical behavior of a physical PV cell while being as simple as possible. During the selection of a PV cell circuit model, a suitable trade-off between accuracy and simplicity has to be determined. Single diode R_p model which is the most appropriate circuit model for PV cells is presented and analyzed in this section. This model is based on five parameters; I_{pv}, a, I_s, R_s, R_p, and illustrated in Fig. 1. Model's I-V characteristic is given by (1), where I_{pv} is the total PV generated current, I and V are the output current and voltage of PV, I_s is saturation current of diode, a is ideality factor of the diode, q is absolute value of the electric charge of an electron, T is temperature in Kelvin and K is Boltzmann constant [46].

$$I = I_{pv} - I_s\left[\exp\left(\frac{q(V+R_sI)}{aKT}\right)-1\right]-\frac{V+R_sI}{R_p} \qquad (1)$$

A PV power converter's main objective is to harvest maximum power from PV beams and send it to the utility grid. In this way, maximum power point tracking (MPPT) algorithms play a significant role in maximizing the yielded power from PV arrays. PV array configuration determines how the power converters and control methods are organized. Several definitions exist on the types of power converters used in grid connection of PV power plants, but the centralized, string and multi-string inverter topologies are the most common. Multiple studies have addressed single-phase and three-phase inverter topologies. Fig. 2 illustrates the most common configurations of PV inverters. The centralized PV inverters are mostly used at high power solar plants where several PV modules are connected in series and parallel to produce combined power. The use of conventional centralized inverters in PV plants has been common for decades because of their high power density and MW conversion capabilities. Large PV power plants are typically interfaced with utility grids using central inverters. Central inverter topologies typically utilize two-level (2L) full bridges or three-level (3L) bridges such as neutral point clamps (NPC), conventional H-bridges (H4), T-types, or emerging voltage source inverter topologies [8]. Utilizing these inverter topologies is primarily driven by the requirement for a single DC bus, which is easily obtained through DC-coupling of PV power plants. In order to avoid overvoltage risks of large PV array strings, the DC bus voltage is typically kept below 1000V limit of PV module insulation and up to 800V.

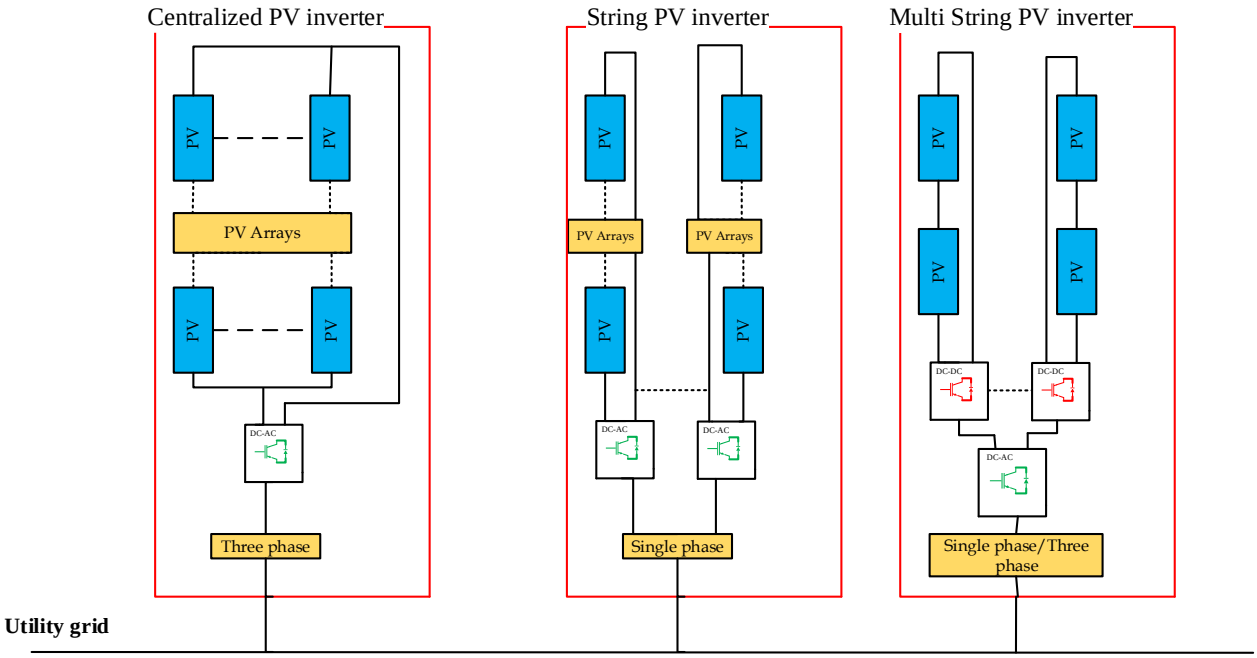

Fig. 2 PV inverter configurations [8].

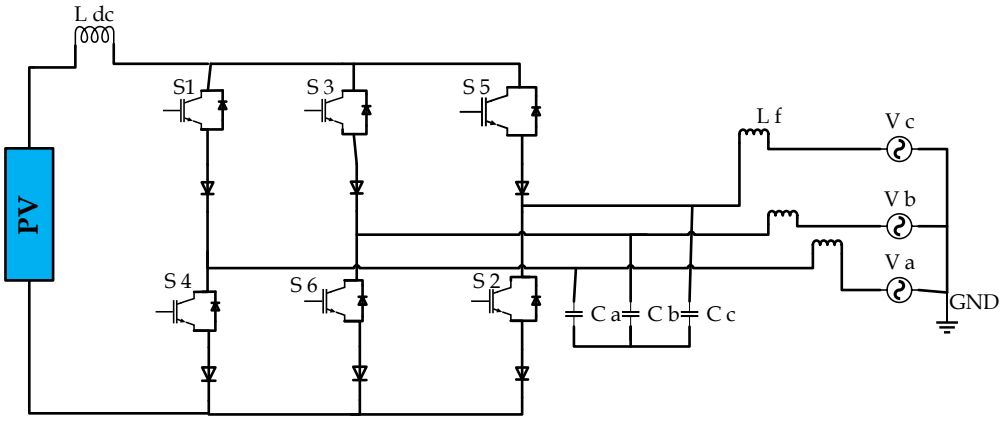

Fig. 3 The topology of the conventional CSI [48].

4 Full-Bridge Based CSIs

A fairly large number of CSIs which are provided in papers are based on full-bridge inventor structure. In this section, these kinds of inverters are investigated.

4.1 Conventional CSI

This kind is the simplest structure presented for converting DC to AC. The three-phase structure of this converter is illustrated in Fig. 3. S1-S6 are the switches, V_a, V_b, and V_c are the voltages of the grid, *Lf* and *Cf* are filter inductor and capacitor filter, respectively. This inverter benefits the general advantages of the current source inverters such as good gain, short circuit protection, one stage power conversion, acceptable lifetime and etc. In addition to its advantages, this inverter has disadvantages like low efficiency, which is 73.57%, and a common-mode voltage generating that causes common-mode current leakage [21]. The maximum amount of common-mode leakage current for photovoltaic systems is 300mA, within 0.3s based on DINVDE 0126-1-1 standard that is summarized in Table 4 [38, 40, 44]. Harmonic components of leakage current in the conventional inverter are more than the maximum limit based on Table 5. So, it is not suitable for a grid power supply photovoltaic system. Also, the switches of the CSIs must be capable of reserve blocking, and this capability can be reached with series-connected diodes to the IGBTs (as shown in Fig. 3); therefore, the semiconductor losses increase. However, recently developed RB-IGBTs in their off states are able to block both reverse and forward voltages, so the series diodes are not needed [21]. These inverters require isolating transformers because of the high level of leakage current in inverters but using them causes low efficiency (reduces overall by 3% [40]), big size, and

Table 4 VDE 0126-1-1 standard for inverters [44].

Leakage current (RMS)	Break time	Grid frequency monitor	Disconnected from the grid within
i > 300 mA	0.3 s	50.2 < f < 51.5	0.2 s
Δi > 30 mA	0.3 s		
Δi > 60 mA	0.15 s		
Δi > 150 mA	0.04 s	f > 51.5 or f <47.5	0.2 s

Table 5 Voltage and current amplitude of parasitic capacitors [21].

Harmonic No.	Frequency [Hz]	Voltage [rms]	Current [A]
3	150	155	0.15
147	7350	75	3.47
150	7500	116	5.47
153	7650	68	3.27

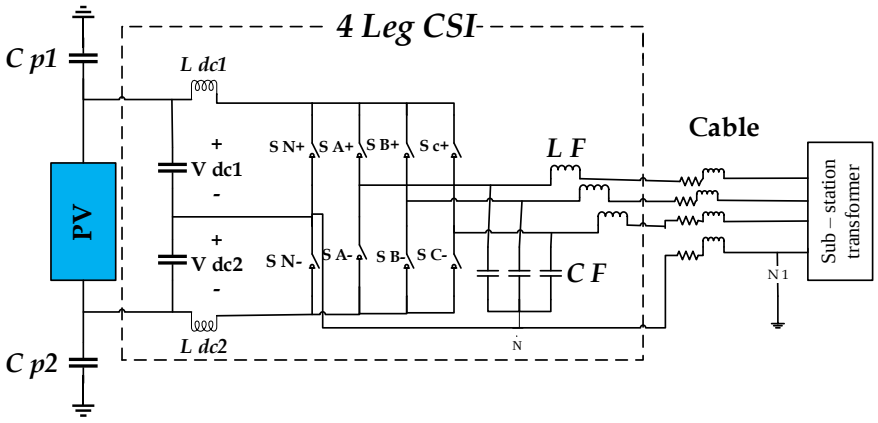

Fig. 4 The 4-leg CSI [21].

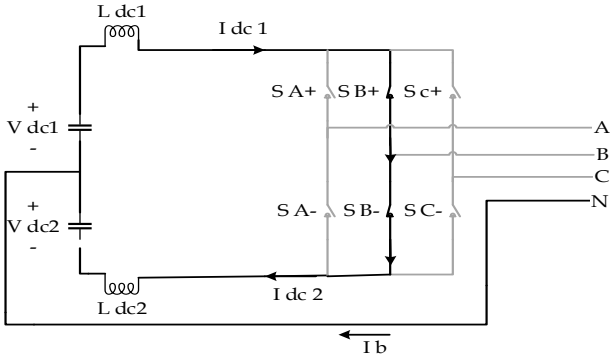

Fig. 5 The current path in connection of two switches [21, 49].

Table 6 Parameters of conventional and four-leg CSIs.

Parameters	Conventional [21]	Four-leg [21]
Power [kW]	10	1.8
Grid voltage [V]	400 rms	380
DC link voltage [V]	300	300
Switching technique	PWM	PWM
Switching frequency [kHz]	-	-
AC filter inductor [mH]	0.4	400
AC filter capacitor [μF]	100	3.3
DC link inductor [mH]	2.1	1.2
DC link capacitor [μF]	25	50

high costs (increases about 25%) [15, 47]. The specifications of a conventional CSI topology are presented in Table 4.

4.2 Four-Leg CSI

This structure, shown in Fig. 4, is three-phase. It reduces current leakage by increasing the impedance of the current path on the DC side by adding two series capacitors that their middle point is connected to the system's null and coupling inductors. Also, these capacitors lower the ripple of DC current. When both upstream and downstream switches are connected to a branch, the current, according to Fig. 5, moves from the intermediate position of the capacitor to the zero points of voltage [21, 49]. In addition, this converter has two more switches compared to the conventional one; power losses of both inverters are equal and, its efficiency is 0.5 KW and in a full load of 2 KW is 97% and 96.4%, respectively. Also, its power factor is 0.99 [21]. Authors in [22] have compared the reliability of this converter with the conventional VSI and CSI in the condition that the RMS amount of the grid's current is 2.583A, THD of the current's waveform is 4.22%, and injected DC current is 10mA [21]. Note: based on IEEE Std.929-2000 standard, the maximum DC current permitted in transformer-less inverters should not be more than 0.5% of the rated current [45, 50], the mentioned DC current value is less than the limit specified in this standard [21]. Finally, they concluded that this one is more reliable. In [21] authors stated that the leakage current of this converter is 159mA, but they have not mentioned its converting gain. The presented method in [21] cause circulating current in the null wire, which affects inefficiency and THD negatively. Also, the balance and equality of the two series capacitors are not guaranteed. The specifications of a 4-leg CSI topology are listed in Table 6.

4.3 Tri-State CSI

Conventional CSIs have a right-half-plane (RHP) zero in their control-to-output transfer function. One of the RHP zero effects is a non-minimum-phase effect that

causes a fall in the inverter output when a step raise is needed in command reference. For improving this limitation, one of the Tri-state CSIs is presented in [23]. The structure of this inverter is shown in Fig. 6(a). An extra switch used in the structure is because of adding freewheeling states to the modes of the inverter to remove the RHP zero of the common CSI; this action improves the dynamic response of the inverter. In the duty ratio of 0.8, voltage gain is 8, and it can reach up to 20 in other circumstances. Leakage current and its reduction are not mentioned. The single phase of this type of inverters is introduced in [51]. The proposed converter and its modulation method have an additional degree of freedom for eliminating the high-frequency common compared to the conventional ones. The grid current THD is reported 3.77% which shows this CSI yields lower THD as it passes the IEEE 519-2014 standard, and The maximum and RMS values of leakage current are reported 140 mA and 28.1 mA, respectively for the proposed CSI in [51] which is far less than the conventional CSI and meets the VDE-0126-1-1 standard. Also, the experimental results confirm that this topology has a significant leakage current reduction capability [51]. In [24], another structure of this type is presented. Fig. 6(b) shows the presented structure. A switching inductor is used instead of a common inductor in this structure. The gain of the presented inverter in [24] is higher than the one

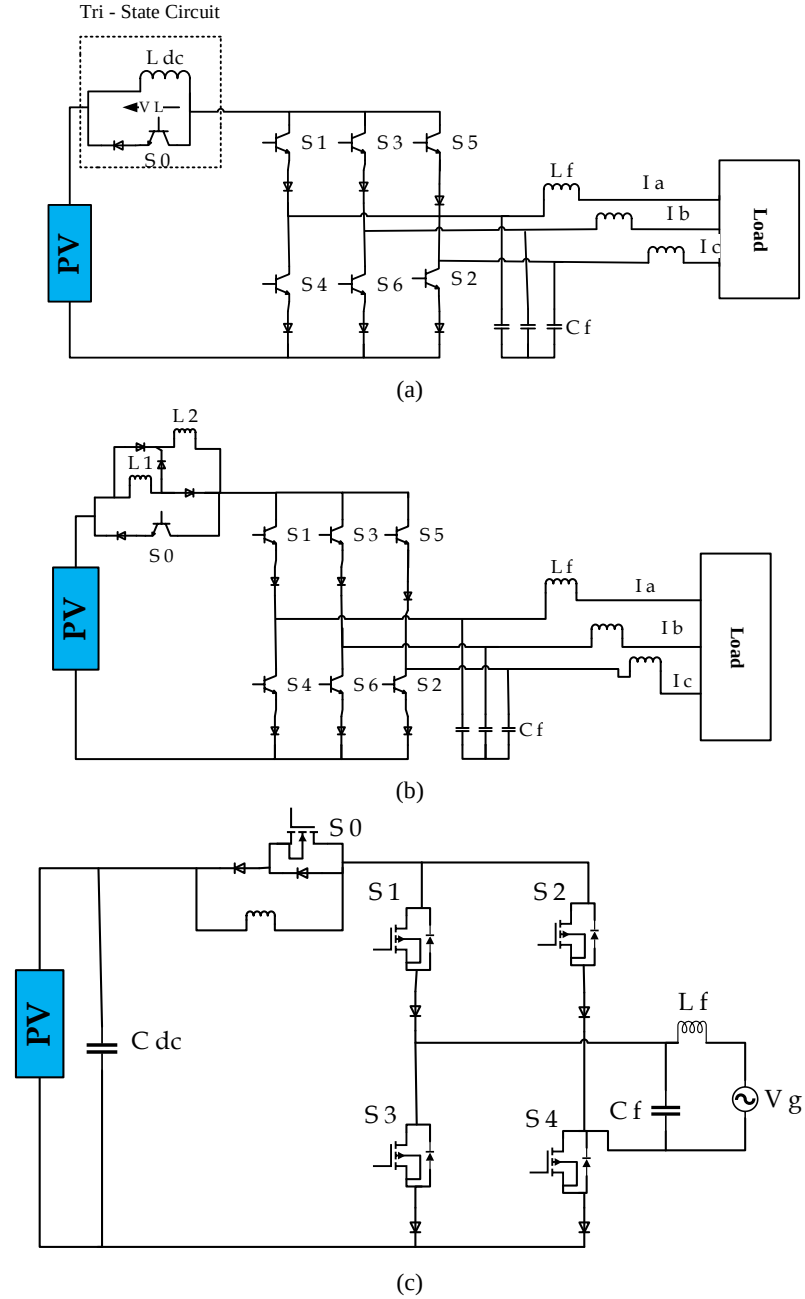

Fig. 6 Tri-state inverter; a) Proposed CSI in [23], b) Proposed CSI in [24], and c) Proposed CSI in [25].

Table 7 Parameters of tri-state CSIs.

Parameters	Tri-state CSI in [23]	Tri-state CSI in [24]	Tri-state CSI in [25]
Power [kW]	-	3.78	1
Grid voltage [V]	375	380	380
DC link voltage [V]	60	102	110
Switching technique	PWM	PWM	PWM
Switching frequency [kHz]	-	-	50
AC filter inductor [mH]	-	8	0.5
AC filter capacitor [μF]	15	1	9
DC link inductor [mH]	20	10	1
DC link capacitor [μF]	-	-	3×1800
Semiconductor	IGBT	IGBT	MOSFET

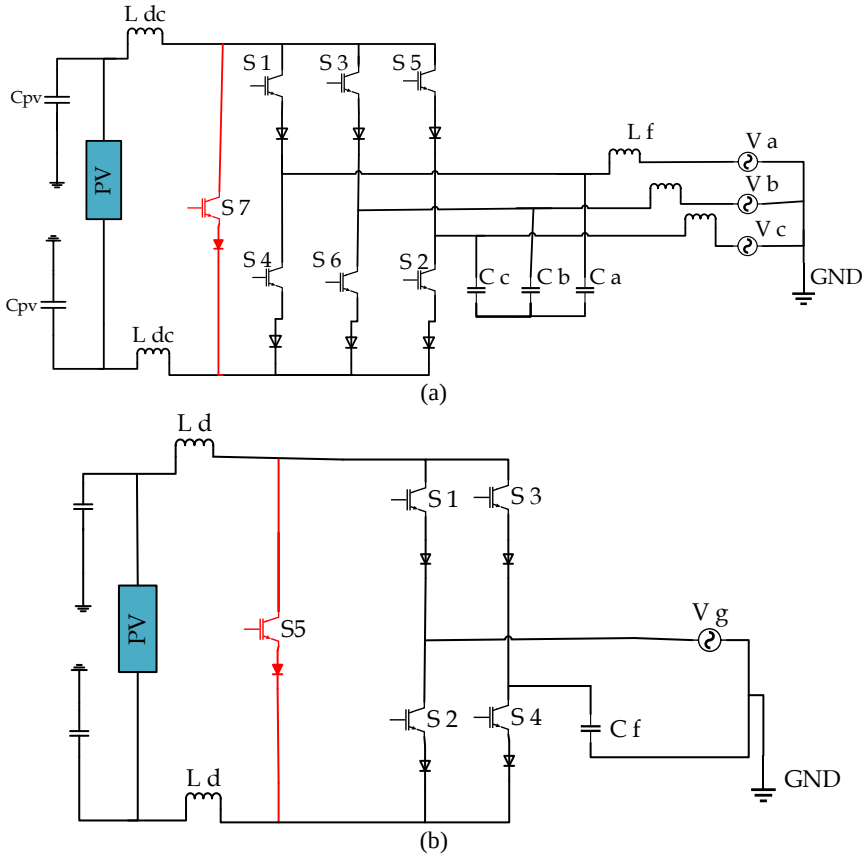

Fig. 7 a) CH7 CSI [26] and b) CH5 CSI [27].

presented in [23]. The gain is almost 14 in the duty ratio of 0.8, and the output current causes acceptable THD. Also, losses and leakage current are not mentioned again. Authors in [25] presented a single-phase kind of the inverter presented in [23]. Fig 6(c) shows this converter. Experimental results show that in a full load of 1kW, the gain of the inverter is about 2 and the THD of output current is less than 2%. In this condition, when the voltage of the solar panel is 110V, the efficiency of the converter is 87.1%. Also, losses are because of conductance losses mostly, which are caused by five switches, diodes, core, and winding of storage inductor. The parameters of the mentioned CSI are listed in Table 7.

4.4 CH7 Current Source Inverter

A three-phase CH7 is presented in [26], and it is shown in Fig. 7(a). This structure uses a parallel switch of the inverter bridge to reduce leakage current. Switch S7 suppresses leakage current by reducing the amount of *dv*/*dt*, which is proportional to the quantity of leakage current. The leakage current reduction is searched in [26], and it is 200mA for the common-mode state in an experimental sample. This structure and suitable control reduce the losses, especially conductance ones, but there is no mention of the efficiency range and converting gain [26]. Note that one of the other advantages of these parallel switches (S7and S5) is to prevent overvoltage. If there is overvoltage, the parallel switch will be turned on until the fault is eliminated. Therefore, it is safe against open-circuit at dc side. As a result, this provides safety against overvoltage [27]. The Single-phase structure of this converter is presented in [27]. Fig. 7(b) shows the single-phase circuit, in which the RMS

Table 8 Parameters of CH7 and CH5 CSIs.

Parameters	CH7 CSI [26]	CH5 CSI [27]
Power [kW]	-	-
Grid voltage [V]	-	-
DC link current [I]	8	8
Switching technique	-	-
Switching frequency [kHz]	10	5
AC filter capacitor [μF]	66	44
DC link inductor [mH]	5	8
parasitic capacitance [nF]	220	56
Semiconductor	IGBT	IGBT

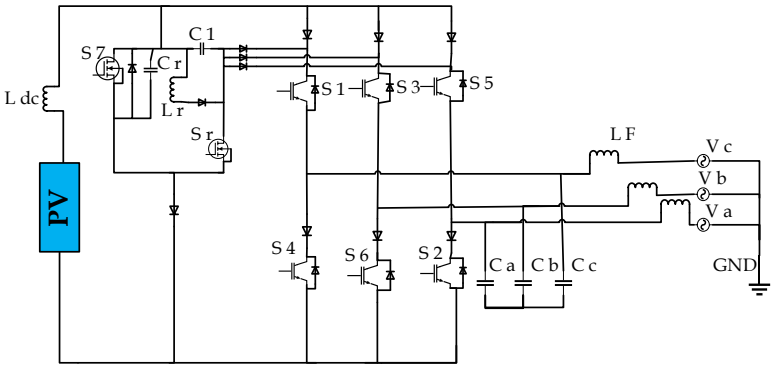

Fig. 8 Soft-switching H7 CSI [48].

amount of leakage current and THD are 24.7mA and 2.69%, respectively. For future applications, the switching frequency tends to be much higher with GaN and SiC devices. Therefore, because of the high switching frequency, the dc-side inductor would be much smaller than in this case. The effect of this issue on leakage current needs more investigations [27]. The switching stress of parallel switches is much more than the stress of other switches that this is a drawback of these inverters [48]. The parameters of CH7 and CH5 are listed in Table 8.

4.5 Soft-Switching H7

As mentioned earlier, high switching stress on parallel switches is a drawback of hard-switching H7. In high-frequency operations switching loss rises; hence Soft-Switching topologies have been introduced to improve these challenges [48, 52]. Several soft-switching VSIs have been introduced in recent years, but most of them suffer from much more cost and space than they need compared to hard-switching VSIs. In contrast, soft-switching CSI has a limited number of species. The structure of Soft-Switching H7 is presented in [48] and shown in Fig. 8. The circuit benefits the S7 switch on the DC side, and also it has an auxiliary circuit for soft-switching. As seen in Fig. 8, a resonant auxiliary switch Sr is used to aim the primary switch (S7) to achieve soft-switching capability. The series-connected resonant inductance Lr with the auxiliary switch and resonant capacitor Cr make a resonant tank together. Diodes D9, D10, D11, and D12 are used to release the energy of Lr to output loads. Diode D7 is set to improve the ability of the current reserve blocking of switch S7. Also,

Table 9 Parameters of soft-switching H7 CSI.

Parameters	CH7 CSI [48]
DC link current [I]	10
Load resistance [Ω]	45
Switching frequency [kHz]	10
AC filter capacitor [μF]	30
Resonant inductor [μH]	18
Resonant capacitor [nF]	10
Semiconductor	IGBT

Capacitor C1 is used for energy absorption. Therefore, switch S7 turns on in zero current and turns to be off in zero voltage, and switching of S7 occurs in zero voltage. Investigation of one cycle of waveforms shows that switching of 6 switches of the bridge-inverter is done at zero voltage. The efficiency is 87.21% which is about 14% more than the conventional one, but there is no statement about VTR, size, and power density. Also, additional diodes, inductors, and capacitors increase the cost and complexity of the circuit. The parameters of soft-switching CH7 are presented in Table 9.

4.6 Other Structures

This section introduces other types of current-source inverters which use the full-bridge circuit with an auxiliary circuit, and the authors have not named them. First, single-phase and then three-phase inverters are studied.

4.6.1 Current Source Inverter With Power Decoupling Capability

There is an oscillation in the output power of the initial current-source inverter, which is two times higher

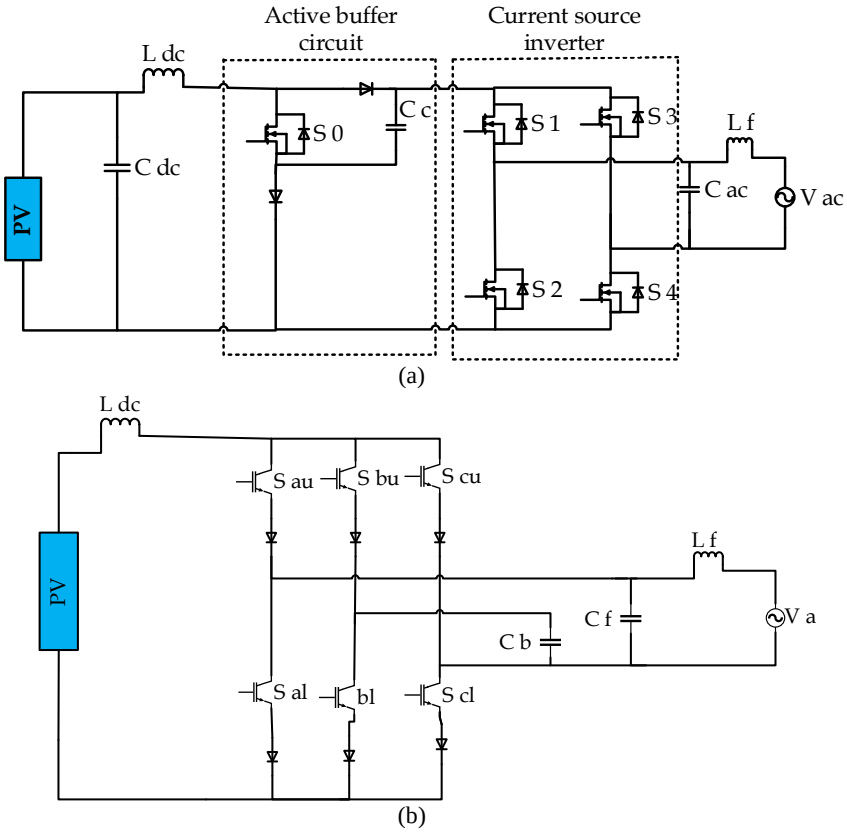

Fig. 9 Presented CSI with power decupling capability in a) [28] and b) [29].

Table 10 Parameters of soft-switching H7 CSI.

Parameters	Presented CSI in [28]
Power [kW]	0.4
Grid voltage [V]	100
DC link voltage [V]	70
Switching technique	-
Switching frequency [kHz]	80
AC filter inductor [mH]	1
AC filter capacitor [µF]	3.3
DC link inductor [mH]	1
DC link capacitor [µF]	3.3
Buffer capacitor [µF]	50
Semiconductor	MOSFET

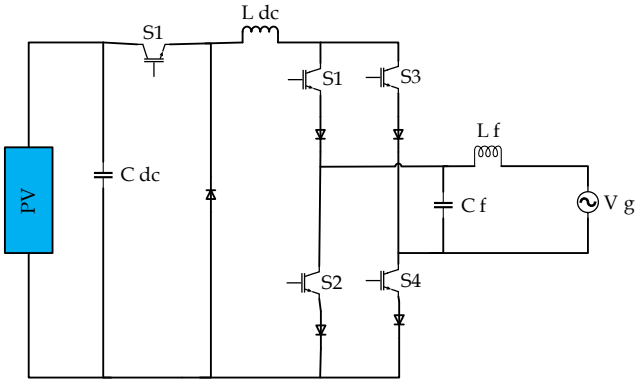

Fig. 10 Proposed CSI in [30].

than the frequency of the grid. So large electrolytic capacitors are used in input to limit these oscillations. In [28], a power decomposer circuit is used that is named active buffer. It is shown in Fig. 9(a). These buffers make small capacitors to control power oscillations; hence the output current with unity power factor and THD of almost 4.24% is achieved. In addition, the active buffer allows DC voltage control to complete the MPPT process. According to the experimental results, maximum efficiency and VTR are 94.9% and 1.43, respectively. Power density is 4.86 in switching frequency of 80 kHz. However, the voltage stress on switches of the filter circuit and the complexity of the circuit are its disadvantages. The presented single-phase inverter in [29] is shown in Fig. 9(b), decomposes the power by a three-phase bridge and a capacitor in output; this is done for removing the power oscillations, which are two times higher than the frequency of the grid. This causes a reduction in the size of the passive elements of the circuit, which improves tracking of the maximum power point. However, it cannot decompose the power when a fault occurs until it relieves. Increasing losses, cost, and circuit complexity are disadvantages of the presented inverter. The parameters of this CSI are presented in Table 10.

4.6.2 An Interface Inverter for Low Voltage PV Application

A current source inverter for connecting solar panels to the grid is presented in [30] and is shown in Fig. 10.

This inverter is capable to connect the low voltage PVs to the grid without using transformers or extra increasing inverters. The proposed inverter has the capability to maintain inductor charge which causes precise control of input inductor and output currents. In addition, one of the other advantages of this CSI is a sinusoidal current injection to the grid by tracking reference current. It is also, capable to track the maximum point of power. THD of the output current is achieved to be 3.1% with a suitable control method. This inverter generates the maximum output voltage of 380V from 280V of the input. Considering mentioned advantages proposed system has high reliability, lower cost, and high efficiency. However, the authors didn't mention anything about leakage current and efficiency. The specifications of CSI topology are listed in Table 11.

4.6.3 Universal Inverter

This kind of inverter presented in [31] and [62] is shown in Fig. 11(a). Although this inverter has a similar structure to the presented inverter in [30], the circuit is able to operate in buck, boost, and buck-boost modes under different switching patterns. This CSI works in DCM mode to change its operation mode (for example, when its mode changes from buck mode to boost). Fig. 11(b) shows another type of these inverters in which the switches are connected to series diodes and the inverter has two inputs; one is connected to a PV, while the other is connected to a fuel cell. This inverter structure increases reliability by replacing fuel cells instead of PV in the absence of sunlight [31, 61]. By using the P&O algorithm, the efficiency is around 99.8%. For a THD of 3.9%, the efficiency is about 78%, and for a THD of 2.1%, the system efficiency is 86%. Therefore, these results show that with decreasing THD, the efficiency increases [31].

4.6.4 CSI5 Inverters

Authors in [32] introduced a single-phase photovoltaic micro inverter based on CSI topology. Fig. 12 shows the structure of the presented converter. An additional key (Sfc) before the full-bridge circuit and two transistors (Sad1, Sad2) reduce the leakage current significantly.

Table 11 Parameters of proposed CSI in [30].

Parameters	Presented CSI in [30]
Power [kW]	-
Grid voltage [V]	280
DC link voltage [V]	310
Switching technique	-
Switching frequency [kHz]	20
AC filter inductor [mH]	3
AC filter capacitor [μF]	2
DC link inductor [mH]	30
DC link capacitor [μF]	-
Semiconductor	IGBT

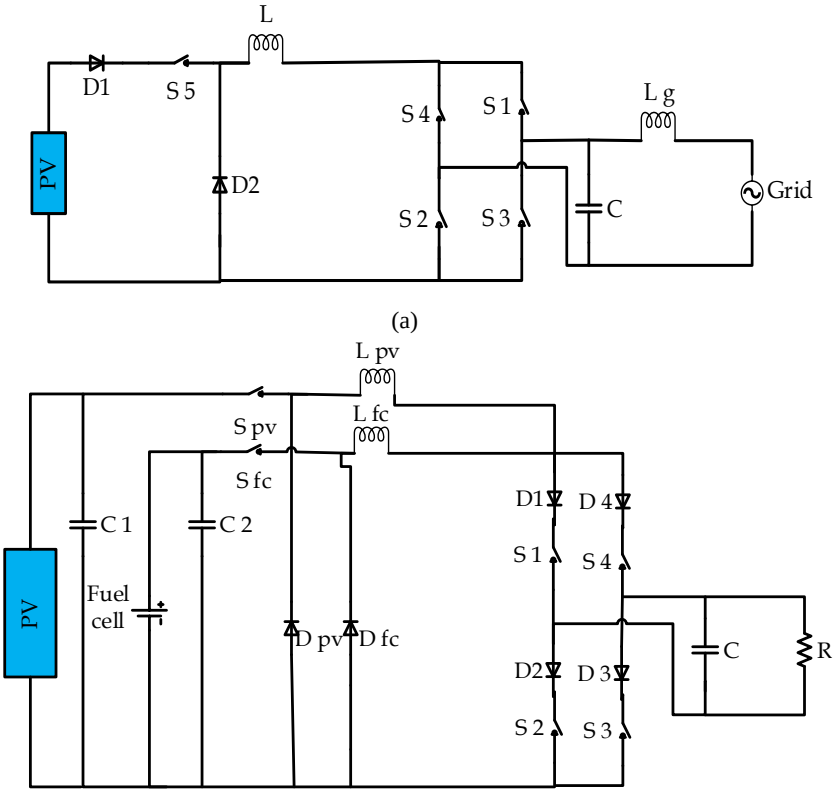

Fig. 11 Universal CSI a) presented in [31] and b) with dual input [31].

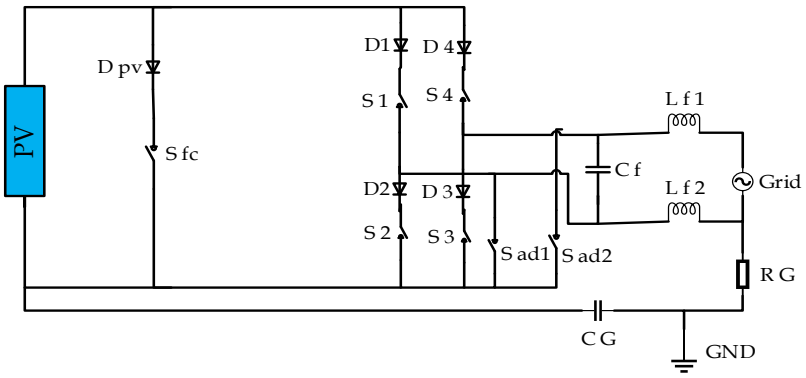

Fig. 12 Presented CSI5 inverter in [32].

Table 12. Parameters of CSI5 [32]

Parameters	CSI 5 [32]
Power [kW]	-
Grid voltage [V]	230
DC link current [A]	1.55
Switching technique	PWM
Switching frequency [kHz]	30
AC filter inductor Lf 1,2 [mH]	0.5
AC filter capacitor [μF]	2.2
Ground resistance [Ω]	3
Equivalent PV parasitic capacitance CG [nF]	330
Semiconductor	IGBT

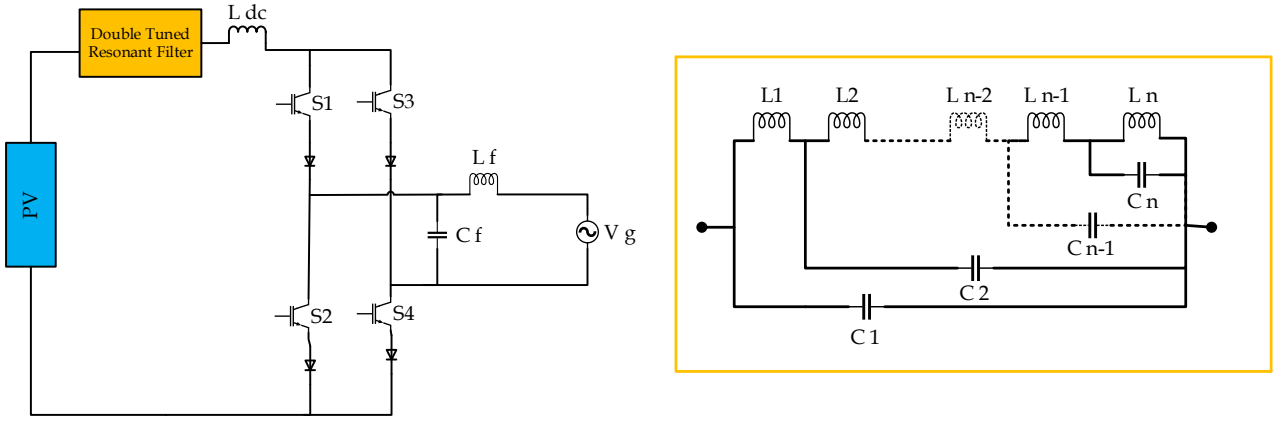

(a) (b)

Fig. 13 a) Presented CSI in [18] and b) A passive filter in input [18].

This is specified by the variation of the voltage that is shown in Fig. 10. The simulation results show that the RMS amount of the leakage current is 27mA. Many semiconductor switches used in the presented structure are its disadvantage, which causes high loss and hardness of control. The authors have not mentioned anything about VTR, which is most noticeable in the field of the application of photovoltaic systems. Table 12 summarizes the parameters of CSI5.

4.6.5 Inverter With a Passive Filter in Input

Authors in [18] have used a circuit for eliminating even harmonics that include inductor and capacitor in the input side. The even harmonics in the input current exist because of the variation of output power. Their frequency is two times higher than the grid's frequency [18]. The presented inverter is shown in Fig. 13(a). Two hardware methods can limit even harmonics. The conventional method is to use a larger inductor in input, and another approach is using a passive filter which is stated above. This circuit which is shown in Fig. 13(b) is capable of removing every even harmonic by adding a capacitor and an inductor for each step. This paper has used two methods for removing second and fourth harmonics. However, the added circuit utilize inductors in size of about 5mH and 10mH. In the low modulation index, THD of the current with a passive filter and a large inductor equals 1.29% in both modes, but it is equal to 2.72% and 6.16%, respectively,

in the high modulation index. It is concluded that passive filters are suitable for PV applications. The efficiency of the converter is 95%, and the power factor is almost unit. Although VTR is not mentioned, this value is 2.2 from the simulation results. The specifications of CSI topology are listed in Table 13.

4.6.6 High-Voltage Ratio CSI

An inverter with an active sub-circuit is presented in [53], which reduces the energy storage switch turn-off voltage spike while it turns off. The presented inverter is shown in Fig. 14. The sub-circuit used in the inverter consists of an inductor with a middle point which makes it two coupling inductors. This inductor is storage. VTR depends on the operation cycle of the storage switch and the tap of the inductor. The presented inverter generates the output voltage of 380 from the input voltage of 96, which shows VTR is about 4.2. Experimental results indicate that the efficiency in full load is 93.48% and the THD of output current is 2.68%. Although MPPT is considered, there is nothing about reducing leakage current. However, voltage regulation is possible with the variable winding ratio of an inductor; the existence of that with added capacitors in the input increases the size and cost of the inverter. The specifications of CSI topology are listed in Table 14.

4.6.7 Four-Leg CSI With Common-Mode Voltage Suppression Capability

An inverter similar to the one in [21] is presented in [54], which has two extra parallel switches with a full-bridge circuit. Common-Mode Voltage (CMV) is a significant challenge in CSIs. This voltage cause leakage current in solar panels [54, 55]. The proposed four-leg CSI is able to significantly reduce the common-mode voltage by a new space vector modulation. In [54], the relationship between switching states and common-mode voltage is investigated, and then it has been concluded that the CMV peak value will be twice

Table 13 Parameters of proposed CSI in [18].

Parameters	Presented CSI in [18]
Power [kW]	0.5
Grid voltage [V]	110
DC link voltage [V]	80
Switching technique	PWM
Switching frequency [kHz]	4
AC filter inductor [mH]	1
AC filter capacitor [μF]	20
DC link inductor [mH]	5
Resonant filter capacitor C1 [μF]	125
Resonant filter capacitor C2 [μF]	250
Semiconductor	IGBT

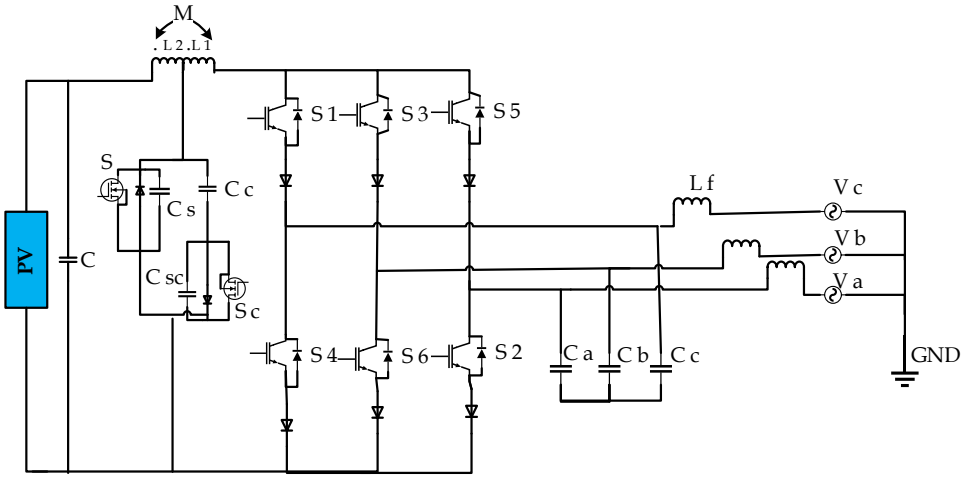

Fig. 14 Proposed CSI in [53].

Table 14 Parameters of proposed CSI in [53].

Parameters	Presented CSI in [53]
Power [kW]	3
Grid voltage [V]	380
DC link voltage [V]	96
Switching technique	SPWM
Switching frequency [kHz]	30–60
AC filter inductor [mH]	0.6
AC filter capacitor [μF]	7.9
Energy storage inductor [mH]	0.612
N2/N1	48/24
Clamping capacitor Cc [μF]	0.44
Resonant filter capacitor C2 [μF]	250
Semiconductor	IGBT and MOSFET

if any zero vector is involved; therefore, by avoiding the zero vector, the common can be suppressed. the relation between switching states and common-mode voltage in zero vectors is presented in Table 15, which shows the value of CMV decreases by using Q6, Q7 switches and replacing the previous three zero vectors (I_1, I_2, or I_3) with I_0. This method can solve the conventional active vector modulations, such as the bipolar current pulses and modulation index range limitation [54]. The presented inverter is shown in Fig. 15. This paper includes nothing about the VTR and THD of the output current.

4.6.8 Inverter With Series Capacitors in Each Phase

A current source inverter with a series capacitor on the output side is presented in [56]. The capacitor reduces the AC voltage in the input of the inverter, which is caused by the voltage ripple. The action also reduces voltage tensions. The presented inverter is shown in Fig. 16. The AC current remains in a fixed amount during voltage drop faults. Adding series capacitors makes the output voltage of the inverter controllable. This converter operates in different input voltages. However, the inverter with series capacitors has high conductance losses, just like the conventional CSI.

4.6.9 Inverter With Three Reverse Blocking IGBTs

An inverter based on the full-bridge converter is presented in [57]. Their difference is in the features of the three switches. RB-IGBT (Reverse Blocking-IGBT) switches have weaker switching characteristics. Also, IGBT can be switched faster with a series diode. RB-IGBT switches are used in a negative row (S4, S6, S2),

Table 15 Space vectors, switching states, common mode voltage of the proposed four-leg CSI in [54].

Space vectors	Switching states			CMV
Zero vectors	I1	Q1	Q4	Va
	I2	Q3	Q6	Vb
	I3	Q5	Q2	Vc
	I0	Q7	Q8	0

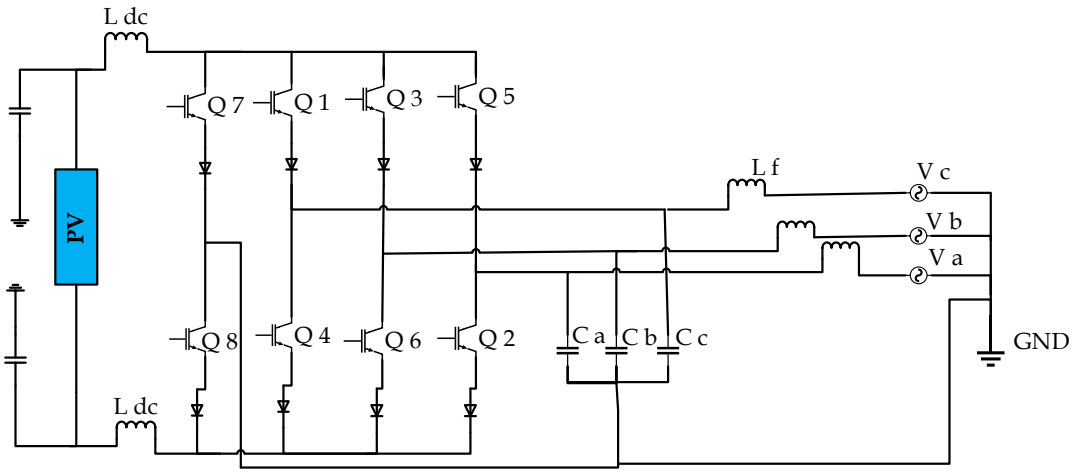

Fig. 15 Proposed inverter in [54].

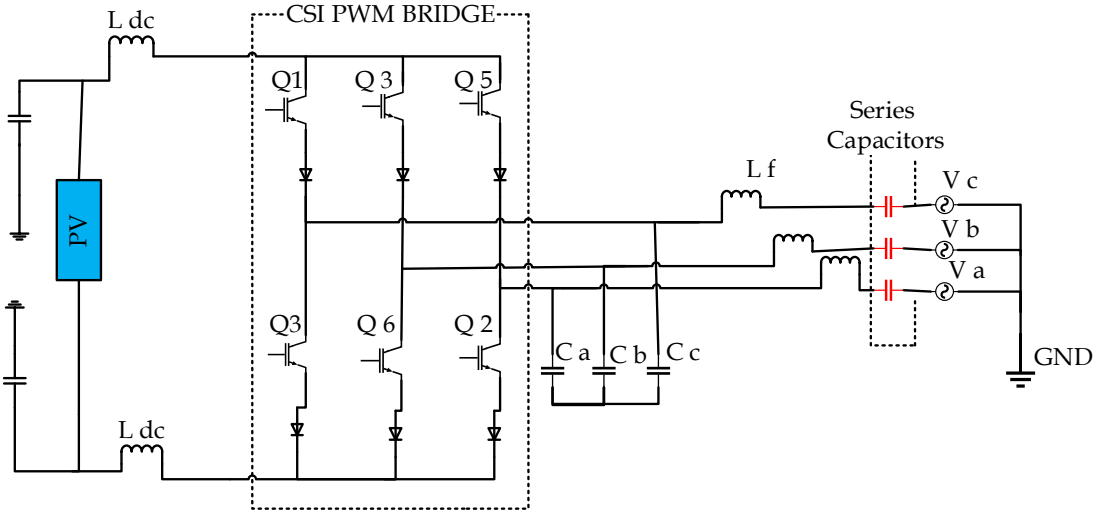

Fig. 16 CSI with series Capacitors in each phase [56].

but the IGBT and series diode are used in a positive row (S1, S3, S5). The converter is shown in Fig. 17. VTR is achieved to be 1.03 in the simulation conditions. However, the conductance losses are less in comparison with the condition that all the switches were RB-IGBT. Moreover, the level of the required switches is lower, and switching losses are less.

5 Specific Structures

A group of current-source inverters does not use the full-bridge circuit structure. This section tries to introduce them.

5.1 Buck-Boost Based CSI

The presented inverter in [58], which is shown in Fig. 18, is a single-stage, high-performance, CSI topology for grid-connected PV systems, which benefits from the boost and buck features. This inverter uses two buck-boost converters. Each of these converters operates in a half-cycle of voltage and in a discrete state. In different environmental situations, the THD of the output current remains less than 5%. According to experimental results that are restricted as per the IEEE-519 standard, the VTR of this inverter is 2.55, which this relatively low VTR is a disadvantage. The specifications of CSI topology are listed in Table 16.

5.2 Cuk Circuit-Based CSI

The most remarkable characteristics of these inverters are that the required inductors and capacitors have a small size, which helps to reduce the size of the circuit and improve its reliability. Fig. 19 shows the position of the Cuk inverters in a three-phase structure. A structure of these kinds of inverters is presented in [59] and [63]. This converter is shown in Fig. 20, and buck and boost is its capability. Also, this inverter receives a continuous current from the input. In the largest operation cycle, VTR is almost 5.5. According to the simulation results, the power factor in this inverter is 0.95, which is less than other inverters. A CSI based on the Cuk converter is presented, which is shown in Fig. 21. Common mode voltage of parasitic capacitors is not differed because of the connection between the null of the network with the negative terminal of the solar panel so, the leakage current will be removed totally [60]. Maximum VTR is 1.4, which is achieved from simulation results; this amount of VTR is less than other circuits, and also THD is less than 3%. The parameters of the proposed CSI in [60] and Cuk circuit are listed in Table 17.

5.3 Differential Buck-Boost Inverter

This kind of inverter has advantages like a low number of switches, the ability to generate a voltage at high level and low level in comparison with the input voltage, better efficiency, smaller size, and low cost. Also, these inverters are capable of operating without large electrolytic capacitors that cause lower reliability. Fig. 22 shows the basic structure of the three-phase buck-boost differential-mode CSI and the location of the differential inverters in the three-phase grid [33].

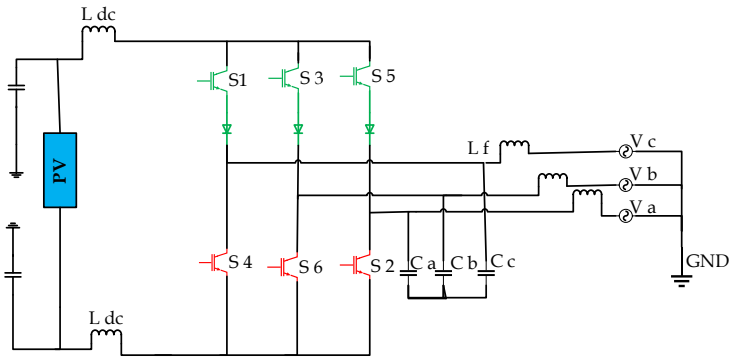

Fig. 17 Presented CSI in [57].

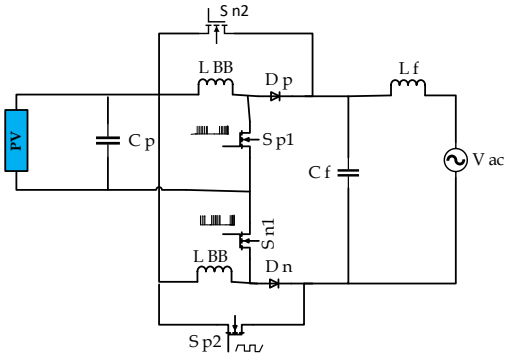

Fig. 18 Buck-boost based CSI [58].

Table 16 Parameters of proposed CSI in [58].

Parameters	Proposed CSI in [58]
Power [kW]	-
Grid voltage [V]	150
DC link voltage [V]	85
Switching technique	SPWM
Switching frequency [kHz]	-
AC filter inductor [mH]	3.25
AC filter capacitor [μF]	4.4
DC link inductor LBB [μH]	20
DC link capacitor Cp [μF]	2000

Table 17 Parameters of Cuk circuit proposed CSI in [60].

Parameters	Cuk circuit [59]	Proposed CSI in [60]
Power [kW]	-	0.5
Grid voltage [V]	50	-
DC link voltage [V]	50	70
Switching technique	PWM	SPWM
Switching frequency [kHz]	50	10
L1 [mH]	1	0.11
C1 [μF]	10	47
C2 [μ F]	-	20
L2 [mH]	1	5
Load Resistance Z [Ω]	1.5	80
Semiconductor	IGBT	IGBT

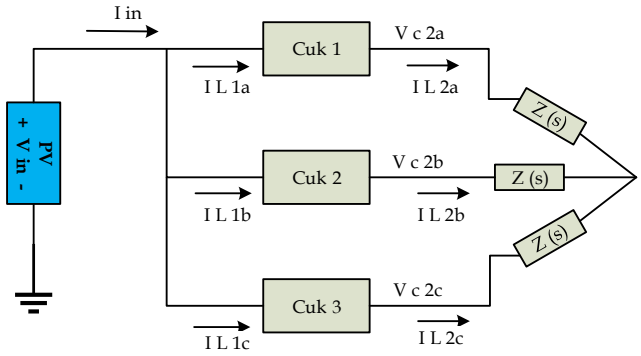

Fig. 19 Locating of the Cuk converters in three-phase structure [59].

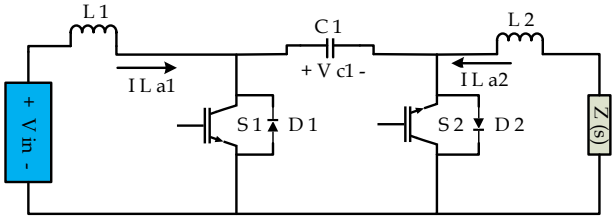

Fig. 20 Cuk circuit structure [59].

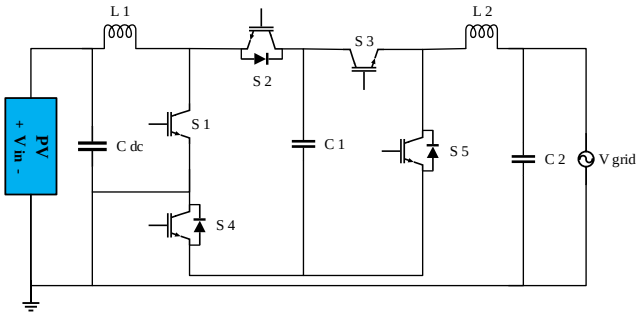

Fig. 21 Cuk circuit- based CSI [60].

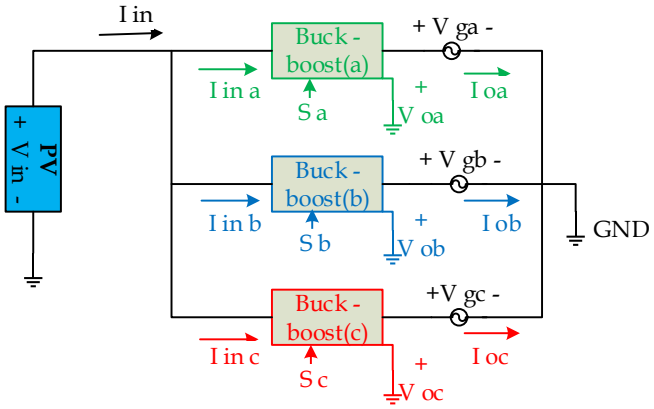

Fig. 22 Location of the differential inverters in the three-phase network.

As shown in Fig. 22, the input dc voltage is connected to three bidirectional buck-boost inverters, also, *Vga*, *Vgb*, and *Vgc* are the grid phase voltages. Using a suitable control algorithm, each of these buck-boost inverters generates an output phase voltage comprised of a sinusoidal pulse width modulated waveform superimposed on a common dc offset component [64]. The dc component in the output voltages is decoupled because of the differential-mode connection of the converter output voltages. The inverters generated output phase voltages are shown as *Voa*, *Vob*, and *Voc* in Fig. 22 and expressed as:

$$Vox = -HxVin \tag{2}$$

$$Hx = \frac{Vox}{Vin} = \frac{Iinx}{Iox} = Hdc + Hac\,\sin(\omega t + \theta) \tag{3}$$

$$Vox = -\left[Vdc + Vac\,\sin(\omega t + \theta)\right] \tag{4}$$

where x = *a*, *b*, or *c*, *H* is the conversion ratio, *Had* and *Hac* are constant values, θ is the voltage arbitrary phase-shift, *Iin* and *Io* are inverters input current and output current respectively.

The possible five topologies of differential-mode buck-boost CSIs without electrolytic capacitors for low-power applications are studied in [33] and shown in Fig. 23. This paper has studied the generic features of the differential inverters. Comparisons show that the best THD in this kind of inverters is 2% which are for the inverters in Figs. 23(a) and 23(c). Also, the minimum ripple of the current is for the inverters shown in Figs. 24(b) and 24(d). The comparison of the DM-CSI inverters shows that the inverters based on C5 and G5 have the least loss and maximum efficiency. However, a large ripple in the input current makes them use a large inductor in the input. The efficiency of the F5 and D1 inverters is acceptable in high input voltages, but it is low in low input voltages. The efficiency of D2

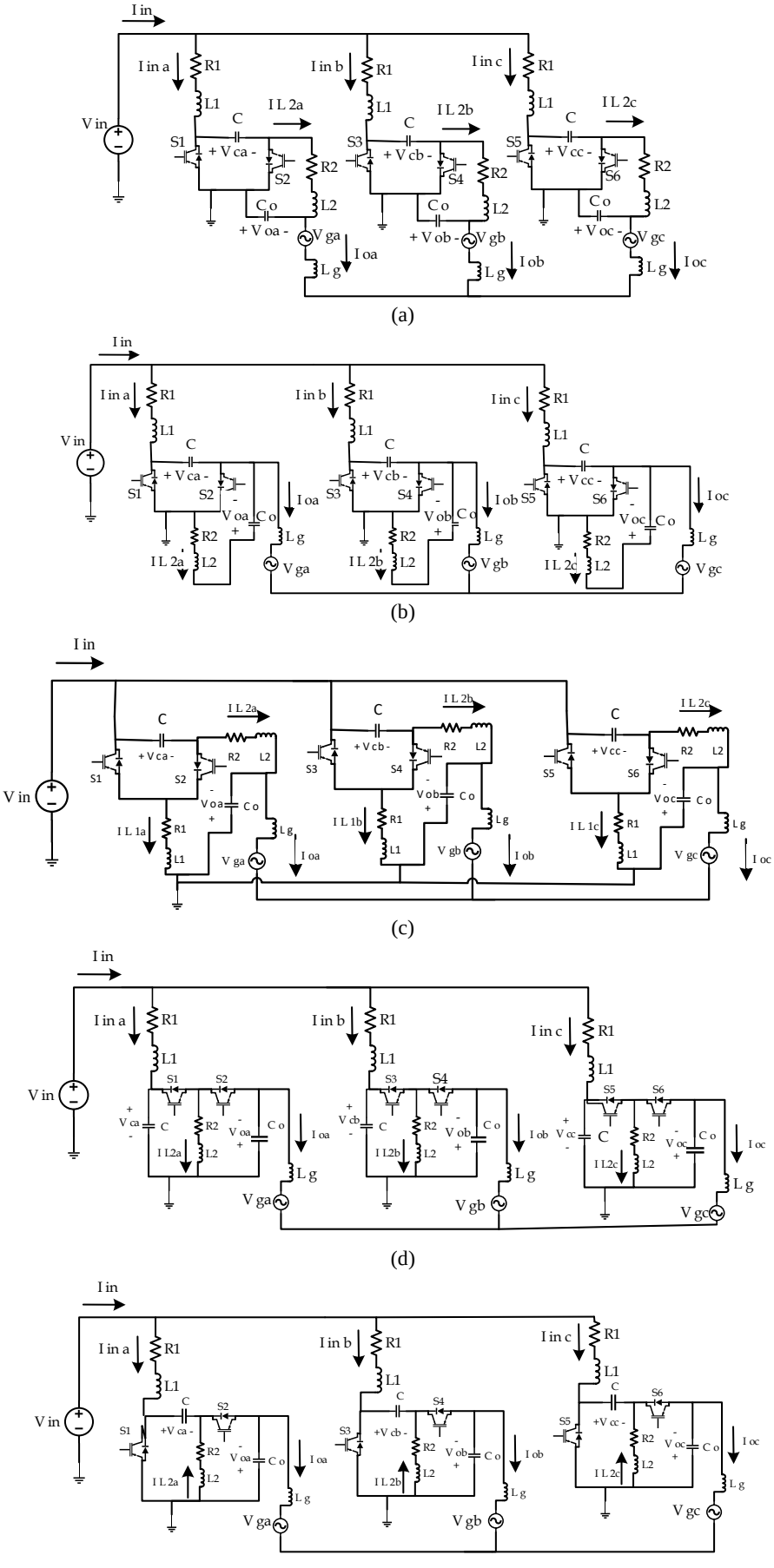

Fig. 23 Differential Buck-Boost inverters [33]; a) C5, b) D1, c) D2, d) F5, and e) G5.

is less than F5 and D1 in high input voltages. The efficiency of D2 is better in low input voltage. G5 and F5 have the least voltage stress, so they use smaller and cheaper capacitors. The size of the proposed inverters depends on the size of elements they have, the size of the inductors is relatively close to the conventional inverters but, the number of capacitors in investigated inverters is more than the conventional ones.

The parameters of investigated Differential Buck-Boost CSIs are listed in Table 18.

Table 18 Differential Buck-Boost inverters [33].

Parameters	Proposed CSIs in [33]
Power [kW]	2.5
Grid voltage [V]	200
DC link voltage [V]	100
Switching technique	-
Switching frequency [kHz]	25
Input inductor	L1 = 1mH, r1 = 0.1 Ω
Output inductor	L2 = 1mH, r2 = 0.1 Ω
Transfer capacitor	C = 10μF
Output capacitor	Co = 2.5μF

6 Comparison Table

A summary of the studies is presented in Table 19. Based on the mentioned table, Conventional CSI has generic advantages like good VTR and protection versus short circuit currents, but it has low efficiency and high current leakage which can make circulation currents. The method of CSI5 reduces current leakage significantly, but a high number of switches increases losses which is related to the conductance of the switches.

Tri-state CSI is the third inverter that is studied. There is an extra switch for changing the modes which improves the dynamic response of the system. High efficiency and low THD for current are its advantages. The losses are mostly because of the conductance losses of the switches.

CH7 inverter uses a parallel switch of the bridge inverter to reduce current leakage, this structure also, reduces the losses. The efficiency of the H7 inverter by using soft-switching is 14% higher than the conventional one. For the inverters which are capable to decompose the power, a decomposer circuit is used for limiting the power oscillation whose frequency is two times higher than the frequency of the grid. In comparison with the initial CSI converters smaller capacitor is used with these buffer controllers. Also, the power factor is unity.

Single-phase interface inverter of low voltage PV can connect low voltage PV to the grid without using a transformer.

Universal inverters are able to operate in buck, boost, and buck-boost modes, which are useful when operating in all of these modes is required.

The inverter with a passive filter in the input is used for removing even harmonics of the current. Passive filters are better than large inductors in high modulation indexes.

The inverter with a series capacitor reduces voltage stress by reducing AC voltage in input, but its conductance losses are high like CSI.

The inverters based on the Cuk circuit are reliable because of the small size of capacitors and inductors. Also, its size is small.

Differential buck-boost inverters have fewer switches, better efficiency, a small capacitor, small size, low cost, and high reliability.

7 CSIs in Future Applications of PV Renewable Energy

Based on an International Energy Agency report, more than 20% of developing countries' populations and almost 1.2 billion people worldwide do not have any access to electricity. Most of them live in rural and under-served remote areas [65-67]. PV systems are considered as one of the suitable ways to provide electricity to the places like remote or off-grid locations [68, 69]. Future Power systems of remote areas will have their own power generation sources and loads, which are considered as micro-grid [70]. For such a power system, the voltage drop is one of the main problems. CSIs that are the interface between solar arrays and micro-grids, due to their voltage-gain feature, help to voltage regulation in the micro-grids of remote areas. In addition, because of having higher reliability than VSI, CSI is a more suitable choice than VSI in remote area power systems suffering from the lack of electrical service companies and experts [71].

One of the PV-based technologies proposed for future applications of PV panels is soar clothing. This technology is introduced to harvest more solar energy to generate electricity, which can be used to supply personal devices such as smartphones or warm-up and cool down the person who wears this cloth [72]. Installed PV planes in cloths are typically thin films that provide low-voltage in their output. Therefore, to provide an effective voltage magnitude, a boost-inverter is needed. CSIs, because of their inherent boosting capability, can be considered an interesting choice for this application. However, to achieve an efficient and effective system for this technology, more investigation into inverters in the future is necessary.

Improving the efficiency of the PV systems is one of the most considered issues by researchers in the last decades. To meet this goal, reducing the amount of material and devices seems to be necessary. In addition, Due to the recent developments in SiC power semiconductor technology, the efficiency and power densities of the CSIs can be increased compared to Si power MOSFET or Si-IGBT based inverters [73].

8 Conclusion

Converters have a significant impact on the reliability and total cost of the PV systems, micro-grids, future

Table 19 Comparison of topologies.

Topologies	Ref.	Leakage current [mA]	THD [%]	Efficiency [%]	Switches and Diodes	VTR	Advantage	Disadvantage	No. of C & L (CSI)	No. of & L (filter)	Scimetric review (No. of published papers)	Price of Converter
Conventional CSI	[47-49]	>300 max	-	73.57	6 Switch	-	Generic advantages of the CSI	Low efficiency. high leakage current and needs isolating transformer	1 L	3 L + 3 C	7600	Low
4Leg	[21, 22, 49]	159 max	4.22	96.4	8 Switch	-	Reduced leakage current and enhance reliability	Voltage equilibrium of capacitors at the input is not guaranteed	1 L + 2 C	3 L + 3 C	1600	Low
Tri – state CSI	[23-25], [51]	-	2	87.1	5 Switch + 5 Diode	2	Improved dynamic response and reduced current THD	Increased the number of Switches	1 L + 1 C	1 L + 1 C	10000	Medium
CH5	[26, 27, 48]	24.7 rms	2.69	-	5 Switch + 5 Diode	-	Reduced leakage current and losses	Use of small inductor in dc-side that could affect leakage current.	2 L	1 C	11800	Low
Soft switching H7	[48, 52]	< 200 max	-	87.21	6 Switch + 12 Diode	-	Increased efficiency rather than the conventional CSI	Increased the number of switches and circuit cost	2 L +2 C	3 L + 3 C	167	Relatively high
The CSI with power Decoupling capability	[28, 29]	-	4.24	94.9	5 Switch + 2 Diode	1.43	A smaller capacitor does power control and PF of output current is unit	High voltage stress on the keys	1 L + 2 C	1 L + 1 C	3600	Medium
Single phase CSI	[30]	-	3.1	High	5 Switch + 5 Diode	1.35	MPPT capability, high reliability and efficiency, low cost and THD, precise output current control	-	1 L +1 C	1 L + 1 C	13100	Low
Universal	[30, 31, 60, 61]	-	2.1	86	5 Switch + 2 Diode	-	Performing buck and boost and buck-boost mode	High EMI	2 L + 1C	1 C	2000	Medium
CSI5	[32]	27 rms	-	-	5 Switch + 2 Diode	-	Reduced leakage current at the output	Increased the number of switches. high losses	-	2 L + 2 C	147	Relatively low
The CSI with passive filter in input	[18]	-	1.29	95	4 Switch + 4 Diode	2.2	Elimination of couple harmonics of input current	Increased final cost due to the use of filter in the input	1 L	1 L + 1 C	2800	Medium
The CSI with high Voltage ratio	[53]	-	2.68	93.48	7 Switch + 6 Diode	3.98	High VTR. voltage regulation	High final cost and circuit size	2 L + 2 C	3 L + 3 C	6000	Relatively high
Buck-boost based CSI	[58]	-	5	-	4 Switch + 2 Diode	2.55	Reduce and increase of voltage, low EMI	Low VTR	2 L + 1 C	1 L + 1 C	11400	Medium
Cuk circuit- based CSI	[59, 60, 63]	0	3	92	5 Switch	1.4	Elimination of leakage current	Low VTR	1 L + 1 C	1 L + 1 C	17500	Relatively high
Differential Buck-Boost inverter	[33, 64]	-	2	-	6 Switch + 6 Diode	2	Low THD, Performing buck and boost and buck-boost mode	have more capacitors than conventional CSI	6 L + 6 C	3 L + 3 C	3300	High

smart grids, etc. Studies in this paper show that recent research has led to the development of current source inverters, improving their advantages and decreasing disadvantages. The most important challenge in current source inverters is the high leakage current which has been reduced in recently developed current source inverters and becomes in the standard range. One of the most important benefits of current source inverters is their high voltage transmission ratio; also, with completing researches, the new generation of current source inverters with higher voltage transmission ratio are introducing. Therefore there will be no need for DC-DC boost inverter and transformer to connect PV panels to the low-voltage grids, especially in low-capacity PV systems (used PV panels in homes) that are developing rapidly; this feature is so important and useful because it leads to higher efficiency and lower cost. This paper provided a review on the current source inverters topologies that have been developed in recent years, which can be useful for selecting the best converter in necessary PV applications and future investigations.

Intellectual Property

The authors confirm that they have given due consideration to the protection of intellectual property associated with this work and that there are no impediments to publication, including the timing of publication, with respect to intellectual property.

Funding

No funding was received for this work.

CRediT Authorship Contribution Statement

N. Danapour: Conceptualization, Writing - Original draft, Writing - Review and editing. **E. Akbari:** Writing - Review and editing. **M. Tarafdar-Hagh:** Supervision.

Declaration of Competing Interest

The authors hereby confirm that the submitted manuscript is an original work and has not been published so far, is not under consideration for publication by any other journal and will not be submitted to any other journal until the decision will be made by this journal. All authors have approved the manuscript and agree with its submission to "Iranian Journal of Electrical and Electronic Engineering".

References

[1] A. M. Alzahrani, M. Zohdy, and B. Yan. "An overview of optimization approaches for operation of hybrid distributed energy systems with photovoltaic and diesel turbine generator," *Electric Power Systems Research*, Vol. 191, p. 106877, 2021.

[2] S. Saeedinia, M. A. Shamsi-Nejad, and H. Eliasi. "A two-stage grid-connected single-phase SEPIC-based micro-inverter with high efficiency and long lifetime for photovoltaic systems application," *Iranian Journal of Electrical and Electronic Engineering*, Vol. 18, No. 2, p. 2355, 2022.

[3] A. Awasthia, A. K. Shuklaa, M. M. SR, C. Dondariyaa, K. N. Shuklaa, D. Porwala, and G. Richhariya. "Review on sun tracking technology in solar PV system," *Energy Reports*, Vol. 6, pp. 392–405, 2020.

[4] J. Liu, J. Wu, X. Zhu, and J. Zeng, "A switched-capacitor multilevel inverter with reduced power components in current loops for renewable energy generation," *Electric Power Components and Systems*, Vol. 47, No. 9–10, pp. 876–888, 2019.

[5] M. Eskandarpour Azizkandi, F. Sedaghati, and H. Shayeghi, "Design and analysis of a high step-up single-switch coupled inductor DC-DC converter with low-voltage stress on components for PV power application," *International Journal of Circuit Theory and Applications*, Vol. 47, No. 7, pp. 1121–1151, 2019.

[6] R. Girish Ganesan and M. Prabhakar, "Non-isolated high step-up interleaved boost converter," *International Journal of Power Electronics*, Vol. 6, No. 3, pp. 288–303, 2014.

[7] J. Mbihi and L. N. Nneme. "A novel control scheme for buck power converters using duty-cycle modulation," *International Journal of Power Electronics*, Vol. 5, No. 3–4, pp. 185–199, 2013.

[8] E. Kabalcı, "Review on novel single-phase grid-connected solar inverters: Circuits and control methods," *Solar Energy*, Vol. 198, pp. 247–274, 2020.

[9] D. Zhaoa, M. Qiana, J. Mab, and K. Yamashita, "Photovoltaic generator model for power system dynamic studies," *Solar Energy*, Vol. 210, pp. 101–114, 2020.

[10] K. S. Teya and S. Mekhilef, "A reduced leakage current transformerless photovoltaic inverter," *Renewable Energy*, Vol. 86, pp. 1103–1112, 2016.

[11] P. Karuppusamy, G. Vijayakumar, and S. Sathishkumar, "Certain investigation on multilevel inverters for photovoltaic grid connected system," *Journal of Circuits Systems and Computers*, Vol. 25, p. 1650108, 2016.

[12] M. A. Hannan, Z. A. Ghani, M. M. Hoque, K. P. Jern, A. Hussain, and A. Mohamed, "Fuzzy logic inverter controller in photovoltaic applications: Issues and recommendations," *IEEE Access*, Vol. 7, pp. 24934–24955, 2019.

[13] N. Danapour S., M. Tarafdar Hagh, S. H. Hosseini, "Integrated wind turbines and power transmission line: A novel concept," *Sustainable Energy Technologies and Assessments*, Vol. 52, p. 102174 2022.

[14] K. Sayed, M. Abdel-Salam, A. Ahmed, and M. Ahmed, "New high voltage gain dual-boost DC-DC converter for photovoltaic power systems," *Electric Power Components and Systems*, Vol. 40, pp. 711–728, 2012.

[15] M. Ashraf, "A maximum power-point tracking multiple-input thermal energy harvesting module," *International Journal of Electronics and Communications*, Vol. 121, p. 153231, 2020.

[16] M. Rajeev and V. Agarwal, "Single phase current source inverter with multi loop control for transformerless grid–PV interface," *IEEE Transactions on Industry Applications*, Vol. 54, No. 3, pp. 2416–2424, 2018.

[17] J. Suganthi and M. Rajaram, "Effective analysis and comparison of Impedance Source Inverter topologies with different control strategies for power conditioning system," *Renewable and Sustainable Energy Reviews*, Vol. 51, pp. 821–828, 2015.

[18] B. N. Alajmi, K. H. Ahmed, G. P. Adam, and B. W. Williams, "Single-phase single-stage transformer less grid-connected PV system," *IEEE Transactions on Power Electronics*, Vol. 28, pp. 2664–2676, 2013.

[19] N. M. R. Santosa and V. F. Pires. "Three-phase STATCOM based on a single-phase current source inverter," *Energy Procedia*, Vol. 14, pp. 2102–2107, 2012.

[20] S. Lee, S. Song, S. Park, C. Moon, and M. Lee, "Grid-connected photovoltaic system using current-source inverter," *Solar Energy*, Vol. 82; pp. 411–419, 2008.

[21] S. Anand, S. K. Gundlapalli, and B. G. Fernandes. "Transformer-less grid feeding current source inverter for solar photovoltaic system," *IEEE Transactions on Industrial Electronics*, Vol. 61, pp. 5334–5344, 2014.

[22] K. C. Potdukhe, A. Munshi, and A. Munshi, "Reliability prediction of new improved current source inverter (CSI) topology for transformer-less grid connected solar system," in *IEEE Power Communication and Information Technology Conference (PCITC)*, pp. 373–378, 2015.

[23] L. Poh Chiang, F. Blaabjerg, W. Chow Pang, and T. Pee Chin, "Tri-state current source inverter with improved dynamic performance," *IEEE Transactions on Power Electronics*, Vol. 23, pp. 1631–40, 2008.

[24] M. Mao, Y. Zheng, L. Chang, and H. Xu, "A single-stage high gain current source inverter for grid-connected photovoltaic system," in *9th International Conference on Power Electronics and ECCE Asia (ICPE-ECCE Asia)*, pp. 1902–1907, 2015.

[25] D. Chen, Y. Qiu, Y. Chen, and Y. He, "Nonlinear PWM-controlled single-phase boost mode grid-connected photovoltaic inverter with limited storage inductance current," *IEEE Transactions on Power Electronics*, Vol. 32, pp. 2717–2727, 2017.

[26] X. Guo. "Three-phase CH7 inverter with a new space vector modulation to reduce leakage current for transformerless photovoltaic systems," *IEEE Journal of Emerging and Selected Topics in Power Electronics*, Vol. 5, pp. 708–712, 2017.

[27] X. Guo, "A novel H5 current source inverter for single-phase transformerless photovoltaic system applications," *IEEE Transactions on Circuits and Systems II: Express Briefs*, Vol. 5, pp. 708–712, 2017.

[28] Y. Ohnuma, K. Orikawa, and J. Itoh, "A single-phase current-source PV inverter with power decoupling capability using an active buffer," *IEEE Transactions on Industry Applications*, Vol. 51, pp. 531–538, 2015.

[29] C. R. Bush and B. Wang, "A single-phase current source solar inverter with reduced-size DC link," in *IEEE Energy Conversion Congress and Exposition*, pp. 54–59, 2009.

[30] S. Saeidabadi, S. H. Hosseini, K. Varesi, and M. Sabahi, "A modified grid-connected current source inverter for photovoltaic application," in *6th Power Electronics, Drives Systems & Technologies Conference (PEDSTC)*, pp. 218–223, 2015.

[31] Ankita, S. Kumar Sahooa, S. Sukchaib, and F. Fernando Yanine. "Review and comparative study of single-stage inverters for a PV system," *Renewable and Sustainable Energy Reviews*, Vol. 91, pp. 962–986, 2018.

[32] G. Migliazza, E. Lorenzani, F. Immovilli, and C. Bianchini, "Ground leakage current reduction in single-phase current source inverter topologies," in *IECON 2016-42nd Annual Conference of the IEEE Industrial Electronics Society*, pp. 2325–2330, 2016.

[33] A. Darwish, A. Massoud, D. Holliday, S. Ahmed, and B. Williams, "Single-stage three-phase differential-mode buck-boost inverters with continuous input current for PV applications," *IEEE Transactions on Power Electronics*, Vol. 31, pp. 8218–8236, 2016.

[34] P. Choudhary and R. K. Srivastava, "Sustainability perspectives- a review for solar photovoltaic trends and growth opportunities," *Journal of Cleaner Production*, Vol. 227, pp. 589–612, 2019.

[35] R. O. Bawazir and N. S. Cetin. "Comprehensive overview of optimizing PV- DG allocation in power system and solar energy resource potential assessments," *Energy Reports*, Vol. 6, pp.173–208, 2020.

[36] R. Araneo, M. Grossi, and S. Bertone, "EMC issues in high-power grid-connected photovoltaic plants," *IEEE Transactions on Electromagnetic Compatibility*, Vol. 51, pp. 639–648, 2009.

[37] Z. Ahmad and S. N. Singh, "Comparative analysis of single phase transformerless inverter topologies for grid connected PV system," *Solar Energy*, Vol. 149, pp. 245–271, 2017.

[38] A. Syeda and T. K. Sandipamu, "A novel single-phase multilevel transformerless PV inverter for reduced common-mode current," *Materials Today: Proceedings*, Vol. 5, No. 1, pp. 524–530, 2018.

[39] I. Patrao, E. Figueres, F. González-Espín, and G. Garcerá, "Transformerless Topologies for grid-connected single-phase photovoltaic inverters," *Renewable and Sustainable Energy Reviews*, Vol. 15, pp. 3423–3431, 2011.

[40] M. C. Cavalcanti, F. Bradaschia, P. E. P. Ferraz, and L. R Limongi, "Two-stage converter with remote state pulse width modulation for transformerless photovoltaic systems," *Electric Power Systems Research*, Vol. 108, pp. 260–268, 2014.

[41] F. Faraji, A. Hajirayat, A. A. M. Birjandie, and K. Al-Haddadf, "Single-stage single-phase three level neutral-point-clamped transformerless grid-connected photovoltaic inverters: Topology review," *Renewable and Sustainable Energy Reviews*, Vol. 80, pp. 197–214, 2017.

[42] J. Jana, H. Saha, and K. Das Bhattacharya, "A review of inverter topologies for single-phase grid-connected photovoltaic systems," *Renewable and Sustainable Energy Reviews*, Vol. 72, pp. 1256–1270, 2017.

[43] L. G. B. Genu, L. R. Limongi, M. C. Cavalcanti, F. Bradaschia, and G. M. S. Azevedo, "Single-phase transformerless power conditioner based on a two-leg of a nine-switch converter," *Electrical Power and Energy Systems*, Vol. 117, pp. 105614, 2020.

[44] W. Li, Y. Gu, H. Luo, W. Cui, X. He, and C. Xia, "Topology review and derivation methodology of single phase transformerless photovoltaic inverters for leakage current suppression," *IEEE Transactions on Industrial Electronics*, Vol. 62, pp. 4537–4551, 2015.

[45] S. A. Azmi, K. H. Ahmed, S. J. Finney, and B. W. Williams, "Comparative analysis between voltage and current source inverters in grid-connected application," *IET Conference on Renewable Power Generation (RPG 2011)*, p. 101, 2011.

[46] A. Rezaee Jordehi, "Parameter estimation of solar photovoltaic (PV) cells: A review," *Renewable and Sustainable Energy Reviews*, Vol. 61, pp. 354–371, 2016.

[47] Z. Ahmad and S. N. Singh, "An improved single phase transformerless inverter topology for grid connected PV system with reduce leakage current and reactive power capability," *Solar Energy*, Vol. 157, pp. 133–146, 2017.

[48] W. Wang, H. Mu, Z. Cao, C. Wang, and F. Gao, "Soft-switching H7 current source inverter," in *IEEE 8th International Power Electronics and Motion Control Conference (IPEMC-ECCE Asia)*, pp. 2243–2248, 2016.

[49] K. G. Jayanth, V. Boddapati, and R. S. Geetha, "Comparative study between three-leg and four-leg current-source inverter for solar PV application," in *IEEE International Conference on Power, Instrumentation, Control and Computing (PICC)*, pp. 1–6, 2018.

[50] B. Longa, L. Huanga, H. Sunb, Y. Chena, F. Victorc, K. To Chong, "An intelligent DC current minimization method for transformerless grid-connected photovoltaic inverters," *ISA Transactions*, Vol. 88, pp. 268–279, 2019.

[51] X. Guo, N. Wang, J. Zhang, B. Wang, and M. Nguyen, "A novel transformerless current source inverter for leakage current reduction," *IEEE Access*, Vol. 7, pp. 50681–50690, 2019.

[52] Z. Huang, Q. Li, and F. C. Lee, "Improved three-phase critical-mode-based soft-switching modulation technique with low leakage current for PV inverter application," in *IEEE Energy Conversion Congress and Exposition (ECCE)*, 2019.

[53] D. Chen, J. Jiang, Y. Qiu, J. Zhang, and F. Huang, "Single-stage three-phase current-source photovoltaic grid-connected inverter high voltage transmission ratio," *IEEE Transactions on Power Electronics*, Vol. 32, pp. 7591–7601, 2017.

[54] X. Guo, D. Xu, and B. Wu, "Four-leg current-source inverter with a new space vector modulation for common-mode voltage suppression," *IEEE Transactions on Industrial Electronics*, Vol. 62, pp. 6003–6007, 2015.

[55] M. N. H. Khan, M. Forouzesh, Y. P. Siwakoti, L. Li, T. Kerekes, and F. Blaabjerg, "Transformerless inverter topologies for single-phase photovoltaic systems: A comparative review," *IEEE Journal of Emerging and Selected Topics in Power Electronics*, Vol. 8, pp. 805–835, 2020.

[56] C. Photong, C. Klumpner, and P. Wheeler, "A current source inverter with series connected AC capacitors for photovoltaic application with grid fault ride through capability," in *IEEE 35th Annual Conference of IEEE Industrial Electronics*, pp. 390–396, 2009.

[57] C. Klumpner, "A new single-stage current source inverter for photovoltaic and fuel cell applications using reverse blocking IGBTs," in *IEEE Power Electronics Specialists Conference*, pp. 1683–1689, 2007.

[58] S. Jain and V. Agarwal, "A single-stage grid connected inverter topology for solar PV systems with maximum power point tracking," *IEEE Transactions on Power Electronics*, Vol. 22, pp. 1928–1940, 2007.

[59] A. Darwish, D. Holliday, S. Ahmed, A. M. Massoud, and B. W. Williams, "A single-stage three-phase inverter based on Cuk converters for PV applications," *IEEE Journal of Emerging and Selected Topics in Power Electronics*, Vol. 2, pp. 797–807, 2014.

[60] M. Rajeev and V. Agarwal, "Novel transformer-less inverter topology for single-phase grid connected photovoltaic system," in *IEEE 42nd Photovoltaic Specialist Conference (PVSC)*, pp. 1–5, 2015.

[61] L. S. Garcia, G. M. Buiatti, L. C. de Freitas, E. A. A. Coelho, V. J. Farias, and L. C. Gomes de Freitas, "Dual transformerless single-stage current source inverter with energy management control strategy," *IEEE Transactions on Power Electronics*, Vol. 28, pp. 4644–4656, 2013.

[62] B. S. Prasad, S. Jain, and V Agarwal, "Universal single-stage grid-connected inverter," *IEEE Transactions on Energy Conversion*, Vol. 23, pp. 128–137, 2008.

[63] M. Mao, L. Zhang, L. Yang, B. Chong, H. Huang, and L. Zhou, "MPPT using modified salp swarm algorithm for multiple bidirectional PV-Cuk converter system under partial shading and module mismatching," *Solar Energy*, Vol. 209, pp. 334–349, 2020.

[64] A. K. Pati and N. C. Sahoo, "Adaptive super-twisting sliding mode control for a three-phase single-stage grid-connected differential boost inverter based photovoltaic system," *ISA Transactions*, Vol. 69, pp. 296–306, 2017.

[65] F. Birol, "Africa energy outlook–A focus on energy prospects in Sub-Saharan Africa," *Technical Report*, International Energy Agency, Paris, France 2014.

[66] United Nations. Kyoto Protocol, 2014. https://unfccc.int/process/the-kyoto-protocol/status-of-ratification

[67] M. Hove, M. Ngwerume, and C. K. Muchemwa, "The urban crisis in Sub-Saharan Africa: A threat to human security and sustainable development," *Stability International Journal of Security and Development*, Vol. 7, pp. 1–14, 2013.

[68] S. Kumaravel and S. Ashok, "An optimal stand-alone biomass/solar-PV/pico-hydel hybrid energy system for remote rural area electrification of isolated village in Western-Ghats Region of India," *International Journal of Green Energy*, Vol. 9, pp. 398–408, 2012.

[69] S. Singh, M. Singh, and S. C. Kaushik, "A review on optimization techniques for sizing of solar-wind hybrid energy systems," *International Journal of Green Energy*, Vol. 13, pp. 1564–1578, 2016.

[70] K. Anoune, M. Bouya, A. Astito, and A. B. Abdellah, "Sizing methods and optimization techniques for PV-wind based hybrid renewable energy system: A review," *Renewable and Sustainable Energy Reviews*, Vol. 93, pp. 652–673, 2018.

[71] B Pillot, M Muselli, P Poggi, and J. Batista Dias, "Historical trends in global energy policy and renewable power system issues in Sub-Saharan Africa: The case of solar PV," *Energy Policy*, Vol. 127, pp. 113–124, 2019.

[72] A. Anzalchi and A. Sarwat. "Overview of technical specifications for grid-connected photovoltaic systems," *Energy Conversion and Management*, Vol. 152, pp. 312–327, 2017.

[73] S. Ozturk, P. Poşpoş, V. Utalay, A, Koc, M. Ermiş, and I. Çadırcı, "Operating principles and practical design aspects of all SiC DC/AC/DC converter for MPPT in grid-connected PV supplies," *Solar Energy*, Vol. 176, pp. 380–394, 2018.

N. Danapour received the B.Sc. and M.Sc. degrees in power Electrical Engineering from the University of Tabriz, Tabriz, Iran, in 2018 and 2020, respectively. He is currently director of the Laboratory of FACTS and Power Systems, University of Tabriz, with several published papers. His research interests include FACTS, electromechanical systems, power electronic converters, storage systems, and micro-grids.

E. Akbari was born in Borujerd, Iran, in 1987. He received the B.Sc. and M.Sc. degrees in Power Electrical Engineering from the Mazandaran University of Science & Technology (MUST), Babol, Iran, in 2010 and 2014, respectively. His research interests include power quality and distribution flexible AC transmission system (DFACTS), application of power electronics in power systems, power electronics multilevel converters, Smart grids, harmonics and reactive power control using hybrid filters, and renewable energy systems. He has published more than 125 papers in reputed journals and conferences. He is a contributing reviewer of the AJEEE journal.

M. Tarafdar-Hagh is with the Faculty of Electrical and Computer Engineering of the University of Tabriz, Iran as a Professor of Electrical Engineering. He is a Senior Member of IEEE. His main area of research is renewable energy, micro-grid, power system operation, FACTS, power quality, and power conversion.

© 2022 by the authors. Licensee IUST, Tehran, Iran. This article is an open-access article distributed under the terms and conditions of the Creative Commons Attribution-NonCommercial 4.0 International (CC BY-NC 4.0) license (https://creativecommons.org/licenses/by-nc/4.0/).